1.4 Longitudinal waves

For the guitar string, the most important wave type is the flexural wave running along the string with a relatively slow phase speed (Chapter 1.1). However, additional waves may be generated that all have a significantly higher propagation speed but contain – relatively – little energy. Due to the high propagation speed, already their fundamental frequency is relatively high. Still, theses additional waves are worth a look.

In analyses relating to Fig. 1.11, an anomaly at multiples of about 1,4 kHz showed up time and again. At first, this was interpreted as a pickup resonance, until it transpired from supplementary measurements that this irregularity depended on the length of the string. Consequently, not the pickup but the string had to be the source. For bodies with dimensions that are large compared to the structure-borne wave-length, it is known that both transversal and longitudinal waves can appear, and combination-type waves, as well [11]. In long, thin rods we find, on top of the tension-force-dependent flexural waves, mainly **dilatational waves** (extentional waves) manifesting themselves. Their propagation speed is constant and non-dispersive:

$$c_D = \sqrt{\frac{E}{\rho}}$$ Dilatational wave speed

For solid steel strings the math yields $c_D \approx 5100$ m/s; with 64 cm as string length we calculate a (tension-force-dependent) fundamental frequency of about 4 kHz for this dilatational wave.

In **wound strings**, the longitudinal stiffness depends mainly on the diameter D_K of the core, while the mass depends on the outer diameter D_A. Given a length-specific compliance n' and a length-specific mass m', the propagation speed calculates as:

$$c_D = \frac{1}{\sqrt{n' \cdot m'}} = \sqrt{\frac{E \cdot D_K^2 \pi}{\rho \cdot D_A^2 \pi}} = \frac{D_K}{D_A}\sqrt{\frac{E}{\rho}}$$ Dilatational wave speed with winding

Compared to the former formula, the correction factor core-diameter / outer-diameter needs to be considered, as well: for customary strings this ratio is about 0,32 ... 0,42. With the latter number, the fundamental frequency f the dilatational wave decreases to about 1,3 ... 1,6 kHz, – a good fit to the measurements. Even more precise results may be achieved by including both the filling-factor and the stiffness of the winding in the considerations.

The resonances of the dilatational waves can be clearly seen both in Fig. 1.11 (at multiples of 1,4 kHz) and in Fig. 1.15 (after 3 ms). The following model describes the effects on the transmission: when plucking the string, two transversal waves running in opposite directions are generated (Chapter 1.1). The place- and time-dependent field quantities *force* and particle *velocity* are connected via the transmission-line equations (Chapter 2), and the wave impedance of the transversal wave calculates as about 1 Ns/m. The bridge (with its piezo pickup) represents the line termination, it may be seen as a very stiff spring (operation below resonance). The output voltage of the unloaded piezo pickup is proportional to the *displacement* of the bridge. The latter causes a mode coupling, i.e. a small portion of the transversal wave is converted into a dilatational wave. The input impedance of the dilatational-wave line forms a loading of the transversal-wave line and thus influences the transfer coefficient of the piezo pickup.

The termination impedances of the string are seen, as a first-order approximation, as large compared to the wave impedances (for more detailed considerations, neck- and body-resonances would need to be looked into). The input impedance of an open-circuit dilatational-wave line shows a co-tangent-shaped frequency dependency, including maxima at the multiples of the fundamental frequency of the dilatational wave. At these maxima, the possibility of the bridge acting like a spring is impeded, and its displacement (and thus the sensitivity of the piezo pickup) is reduced.

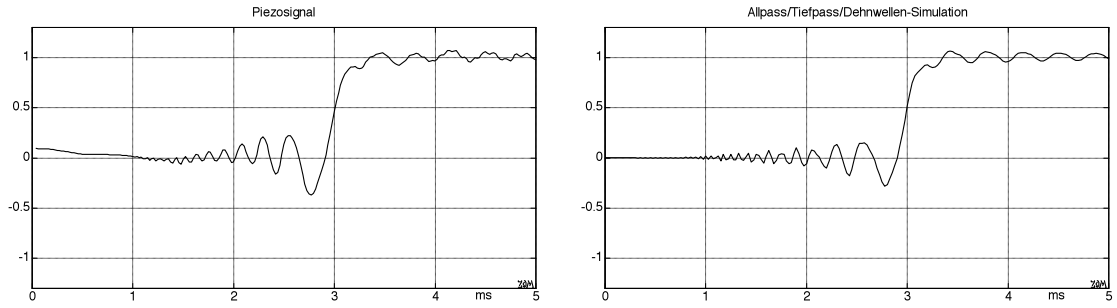

Fig. 1.17: Measurement (left) and dilatational- wave simulation ("Dehnwellensimulation", right); step-excitation at mid-string at $t = 0$, E_2-Saite. "Tiefpass" = low-pass.

In **Fig. 1.17**, the all-pass simulation was supplemented by a dilatational wave, yielding significant improvement. Any remaining differences are due to the plectrum (low-frequency, left-hand section of the figure) and to reflections at the nut (high-frequency, right-hand section of the figure). Both these effects were not included in the simulation.

The principle effect of the dilatational-wave line on the piezo pickup may be described via discrete elements: at very low frequencies, only the longitudinal stiffness acts, and the model system consists of a spring. To emulate the lowest Eigen-oscillation, the mass is thought to be concentrated in the middle of the string with a spring each left and right of it. Above this resonance, the movement of the mass decreases due to the inertia, and half the spring forms the input impedance. To model the higher Eigen-resonances, the string is subdivided into more and more partial springs with interjacent partial masses. A shortening of the spring corresponds to an increase of the stiffness such that the piezo is loaded by a spring with continuously increasing stiffness as the frequency increases. With this, the piezo-sensitivity decreases towards high frequencies in a staircase-shaped manner, with the steps located at multiples of the dilatational-wave resonances.

In the upper section of **Fig. 1.18**, the spectral analysis of Fig. 1.11 is repeated. The low E-string (E_2) was plucked with a plectrum at a distance of about 5 mm from the bridge. The lower section of the figure shows the result of the simulation calculation, with the dispersion-caused inharmonicity, the dilatational-wave loading, and a simple treble damping (1^{st}-order low-pass) being considered. Both sections of the figure show similar irregularities at integer multiples of 1,4 kHz – these can be explained as **dilatational-wave resonances**. The spectral envelope has a similar shape in both graphs, but differences remain in the details. The most important reason for these differences is in the frequency of the partials, the calculation of which was based on an ideal tensioning of the string in the formulas discussed up to now. The real nut and bridge impedances are, however, not infinite: neck, body, neighboring strings, and many small parts all vibrate as coupled parts of a complicated system. This results in a multitude of structural resonances.

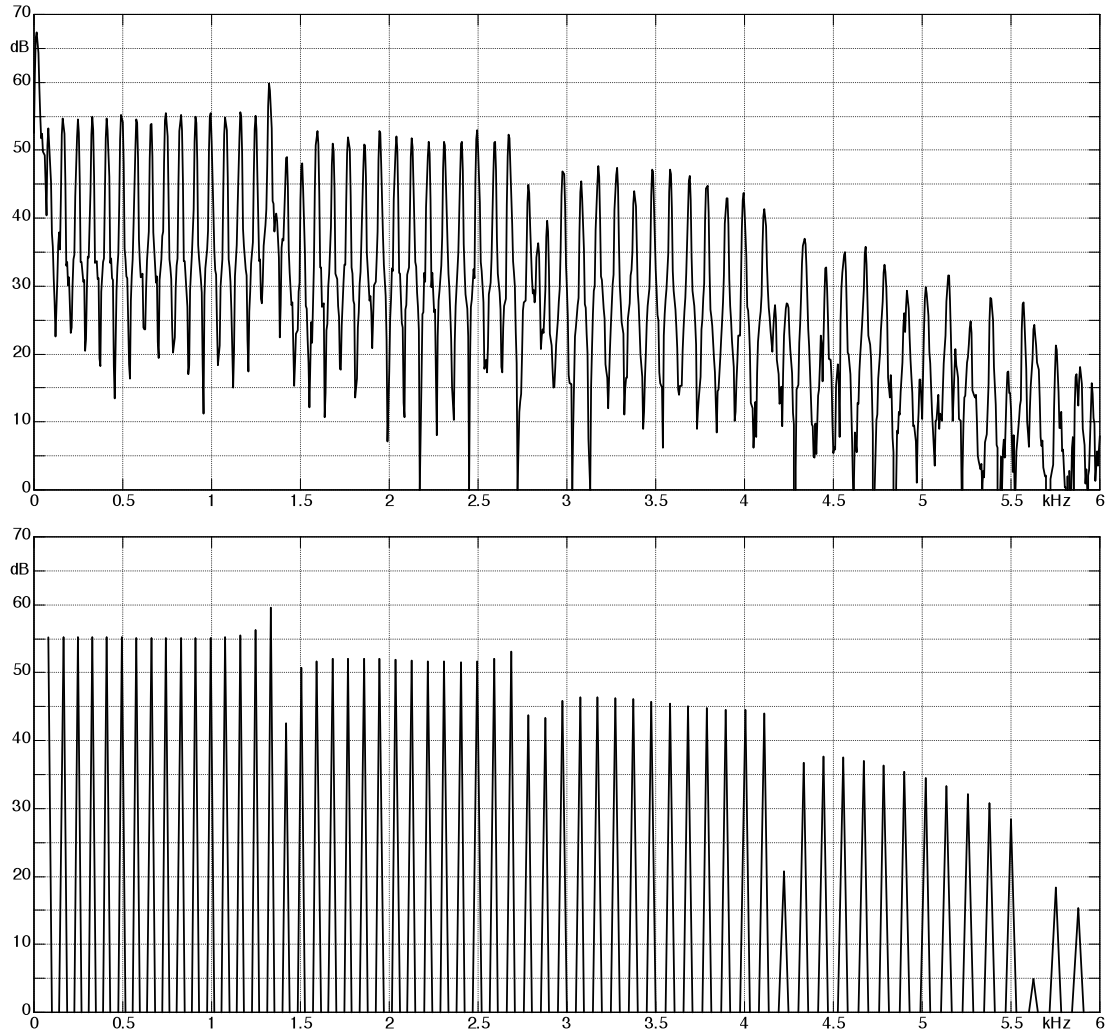

Fig. 1.18: Magnitude spectrum: measurement (top) and model calculation (bottom).

All vibrations may not only appear in one but in three directions – and torsional vibrations are possible, in addition. Not all resonances will substantially influence the bridge impedance but the dilatational waves obviously have a non-negligible effect. In Fig. 1.18, the resonances of the dilatational waves are exclusively considered relative to the frequency response of the piezo (global envelope) – they are not considered regarding their influences on the exact frequencies of the partials (see additional info about this in Chapter 2.5). Because of the high Q-values of the resonances and the connected steep cutoff slopes (dB/Hz), already a resonance-shift of a mere few permille (!) causes a clear change in the levels of the lines. Moreover, additional spectral lines result (clearly visible at 2,8 kHz). The mechanical parameters of a guitar cannot be established with an accuracy of in the permille-range, and thus the limitations of the modeling come into view.

During the investigations, the model based on dilatational waves originated early on as a working hypothesis to explain the step-shaped envelope. Three years later, an experimental setup deploying a laser vibrometer became operational – it delivered further supporting findings:

The laser-based setup consists of stone table weighing in at 250 kg, with a **Polytec laser-head** mounted to it. A steel wire of 0,7 mm diameter is stretched in parallel to the table surface; one end of the wire finds its support in a knife-edge bearing located on a U-brace bolted onto the table surface. The other end of the wire is mounted to an impedance head (Brüel&Kjaer 8001) located on a wall across the hall at a distance of 13,3 m; it measures the longitudinal force. The wire is tensioned such that its fundamental frequency is 5 Hz; given a length of 0,65 m for the string, the equivalent would be a fundamental frequency of 102 Hz. A laser vibrometer sampled the vertical vibration of the wire; the same vibration was also sensed by a pickup mounted under the string on the stone table. This "long string" was excited via a pick made of Pertinax moving downwards in a hammer-like fashion and thus having the effect of a short transversal displacement impulse (**Fig. 1.19**).

With the location of the excitation being close to the bearing of the string, the short section of the string acts like a stiff spring; the long section of the string – with the input impedance being the wave impedance – may be disregarded in comparison. In conjunction with this string stiffness, the mass of the Pertinax pick forms a 2^{nd}-order oscillation system … at least as long as force is being transmitted. Consequently, the string displacement is in the shape of a half-sine in the transversal direction. Fig. 1.19 shows this idealized transversal movement, and also the results of laser-measurements for comparison. Increasing in width due to the dispersion, this half-wave impulse runs along the string as a flexural wave; its group speed (1.3.1) amounts to 133 m/s at low frequencies, and to about three times as much at high frequencies. The first reflection can therefore be expected to be back at the laser vibrometer not earlier than after 66 ms. However, as early as after $T = 5{,}15$ ms, the laser beam measures a reflection that is repeated with decreasing amplitude in equidistant intervals. Given an overall running path of 26,6 m, this yields a propagation speed of $c_D = 5165$ m/s – the typical value for (dispersion free) **dilatational waves** in steel wires.

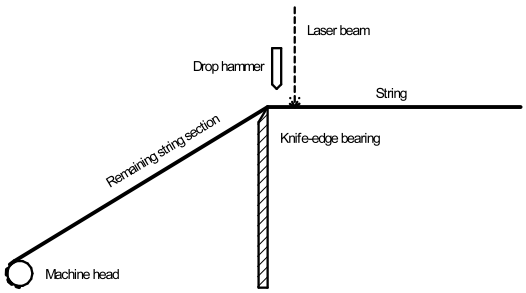

Fig. 1.19: Laser measuring setup (left).
"Wirbel" = machine head; "Saitenreststück" = remaining section of the string; "Fallhammer" = drop hammer; "Schneidenlager" = knife-edge bearing; "Laserstrahl" = laser beam; "Saite" = string;
The graphs shown below depict measuring results of the transversal displacement of the string with different time-axis scaling. Below right: the idealized shape of the curve is indicated as a dashed line and with a horizontal shift. The excitation happens at about 1 mm distance from the knife-edge bearing; the measuring point of the laser is very close to it at 5 mm from the knife-edge bearing.
"Auslenkung" = displacement.

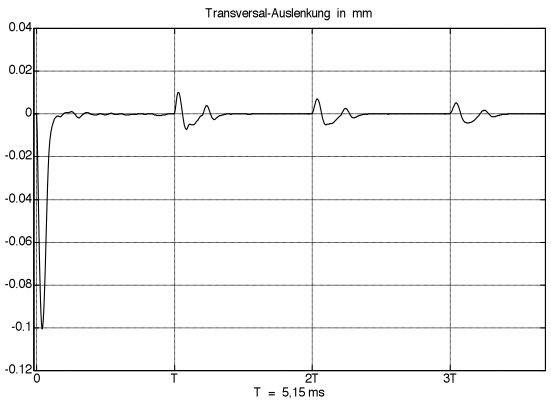

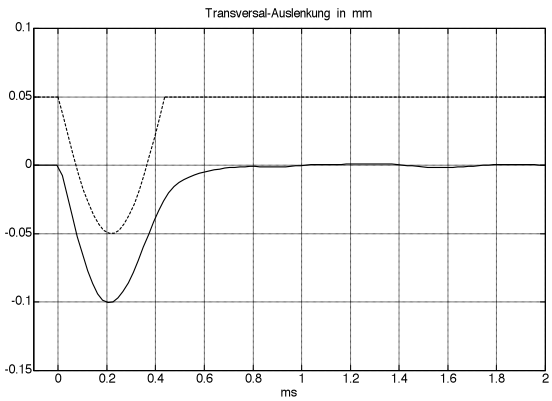

The dilatational wave remains almost invisible to the **laser-vibrometer** because the laser beam can react only to transversal but not to axial movements♣. Periodicities of T = 5,15 ms are nevertheless measured – this is due to a coupling of the two wave types: the string is bent at its bearing, and here the dilatational wave returning after 5,15 ms triggers a secondary flexural wave that is visible to the laser beam.

The measurement results from the laser setup are shown in **Fig. 1.20**, the longitudinal force measured at the end of the string being subject to integration. Without support-bearing, the dilatational wave of the string (having been triggered at the left-hand bearing) reaches the right-hand bearing after 2,6 ms. The excitation impulse is comparable but not identical to the one shown in Fig. 1.19. With the **support-bearing**, the force sensor receives its first excitation after 2,6 ms, as well – there is, however, some attenuation. Without the support-bearing, the second impulse arrives 5,2 ms after the first one, with support-bearing this happens already after 2 ms. The reflection of the longitudinal-force-wave is in phase at both clamps (rigid clamping); at the support-bearing we obtain complex factors for both reflection and transmission. The small ripples visible in the left section of Fig. 1.20 can be traced to unavoidable resonances in the left-hand bearing; they have no special significance.

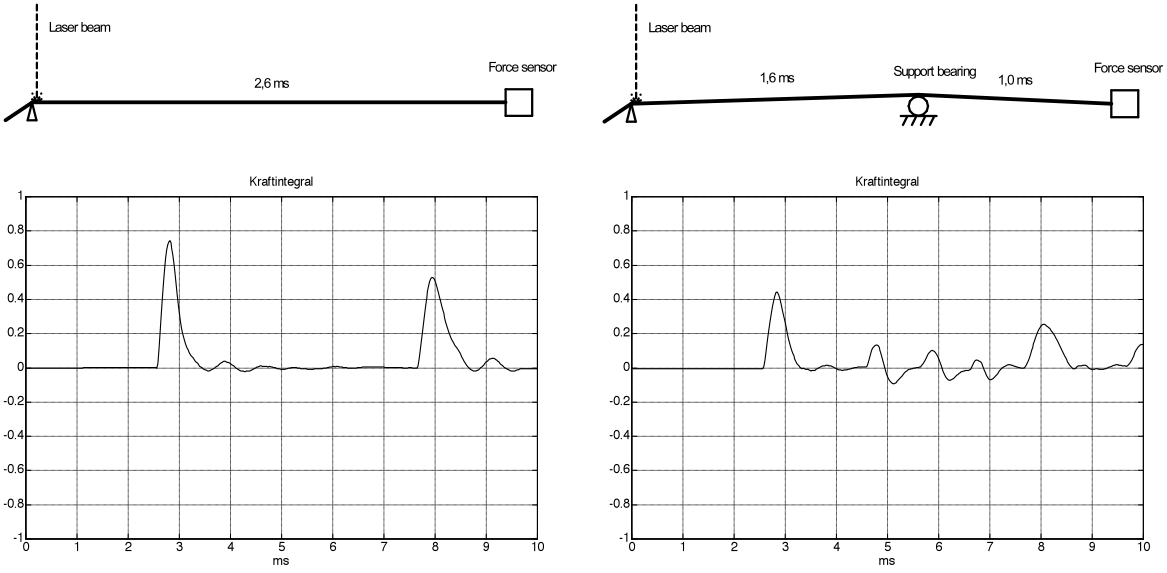

Fig. 1.20: Laser setup with/without support-bearing. The support-bearing separates the string length into two parts 816 cm : 511 cm. The diagrams show the temporal integral of the longitudinal string-force; the unit is Newton · millisecond (Nms). The positive sign indicates that first compression and then strain reach the sensor. "Laserstrahl" = laser beam; "Kraftsensor" = force sensor; "Kraftintegral" = force integral; "Stützlager" = support-bearing.

In the right-hand section of Fig. 1.20, the **reflections** differ (in their shape) from the primary impulse starting at 2,6 ms. Between 4,6 and 7,5 ms, three bipolar impulses can be observed: on its path from the source (at the left-hand bearing) to the force sensor, each of them has traversed the support-bearing once and has additionally received several reflections at the support-bearing. In the case of a uni-polar impulse changing to a bi-polar one, we can assume high-pass filtering. The change of shape of the impulse allowed only for the conclusion that the reflection acts as a **high-pass**, and the transmission as a **low-pass**.

♣ Effects of lateral contraction are too weak.

Fig. 1.21 shows results of calculations using a **dilatation-wave model**. A 1st-order low-pass (cutoff frequency at 1,5 kHz) emulates the transmission across the support bearing, while a 1st-order high-pass (cutoff frequency at 1,5 kHz) models the reflection. The cutoff frequency was determined via "curve-fitting" (vulgo: we tried until we got a match). The agreement is remarkable.

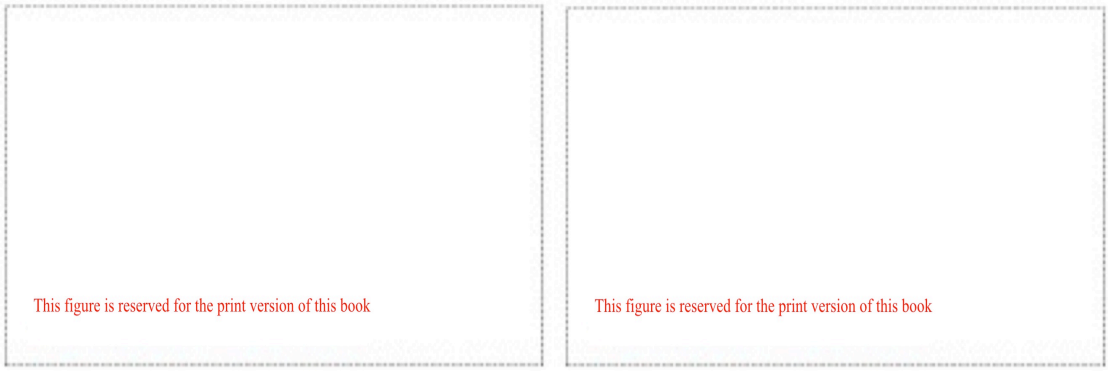

Fig. 1.21: Measurement (left) and model calculation (right); string with support-bearing, as in Fig. 1.20. The time "zero" is shifted by 2,6 ms to the start of the first impulse. The lateral string displacement determined via the laser (close to the left-hand bearing) was used as the input signal for the model calculation.
"Kraftintegral" = force integral.

A movable brass-cylinder (∅ 4 mm) served as **support-bearing** (Fig. 1.20), with the string forming a bend angle of 5° around it. Using the parallel-axes theorem, the axial moment of inertia of a cylinder ($mD^2/8$) can be recalculated into the generatrix moment of inertia ($3mD^2/8$), with m = mass and D = diameter. Longitudinal movements of the string roll the cylinder back and forth on its base; propelling force is the torque $F{\cdot}D$, with F = longitudinal force in the string. With respect to the longitudinal movement of the string, the inertia of the rolling movement of the support-bearing can be recalculated into an equivalent translation using the equivalent mass $m_{ä} = 3m/8$. Here, m is the actual mass of the cylinder (volume x density), and $m_{ä}$ is the equivalent mass to be shifted from the point of view of the string. The source impedance of the dilatational wave arriving at the support bearing is the impedance of the dilatational wave. Given a steel wire of a diameter of 0,7 mm, Z_W is about 15,8 Ns/m (see appendix). The wave transmitted across the support bearing also forms a loading of the latter with Z_W. The support-bearing itself is described via the equivalent mass (**Fig. 1.22**). Using this, the cutoff frequency of the low-pass results as: $f_x = 1/(\pi C R_W) = Z_W/(\pi m_{ä})$, and the equivalent mass may be calculated as 3,4 g. From the latter, the **mass of the cylinder** follows: m = 8,9 g. The cylinder used in the experimental setup indeed had a mass of 8,5 g – the results of the model are nicely confirmed. Whether the cutoff frequency is set to 1500 Hz or 1578 Hz will change the curves in Fig. 1.21 by merely by the width of a stroke.

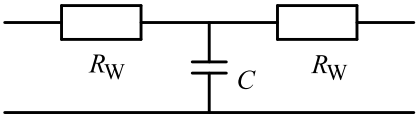

Fig. 1.22: Electrical analogous circuit [3] of the support-bearing. The mechanical wave impedance is transformed into an electrical conductance; the equivalent mass is transformed into a capacitance (FI-analogy).

The reflection- and transmission-processes may also be calculated using the equations for the transversal wave given in Chapter 2.5; in this case the parallel connection of R_W and C needs to be taken for the bearing impedance: $r_F = R_W \cdot pC/(2 + R_W \cdot pC)$. This corresponds to a high-pass HP1.

In order to localize the **origin** of the dilatational wave, the string was plucked at a distance of 51 cm from the left-hand string bearing (**Fig. 1.23**). If already the impact of the drop hammer onto the string would trigger a dilatational wave, then the measured force integral would have to be a dispersion-free image of the string displacement at the location of the origin. However, the result is in fact a better match to the displacement measured closely to the bearing – the only conclusion being that the main portion of the dilatational wave is generated only at the time when the (dispersively broadened) flexural wave has reached the left-hand bearing. This hypothesis is supported by the delay times depicted ion Fig. 1.23, as well.

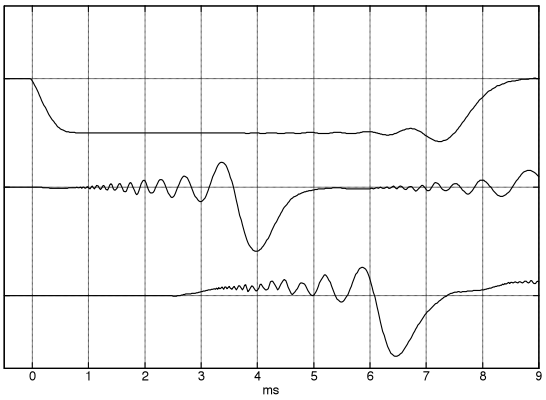

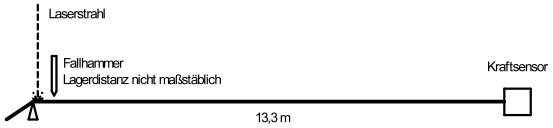

Fig. 1.23: (top to bottom)
- Transversal displacement at the left-hand plucking point,
- Transversal displacement at the left-hand string bearing,
- Integral of the longitudinal force at the right-hand string bearing

Conclusion: dilatational waves merely make for 2nd-order effects on a guitar, but their influence may not be entirely neglected, either. The plucking action mainly generates a flexural wave – but as soon as this hits a bearing (nut, bridge, fret), part of the flexural wave-energy will be transformed into a dilatational wave. Dilatational waves propagate without dispersion and create resonances in the frequency range above 1 kHz. A bearing with a small surface towards the string will only partially reflect a dilatational wave; part of the dilatational wave-energy will be transmitted across the bearing into the other part of the string. The reflected portion manifests itself partially as a dilatational wave and partially as flexural wave.

Fig. 1.24 shows the significance of this **mode-coupling**: a string of 13,3 m length was plucked close to its left-hand bearing, with the laser measuring-point right next to it. At 20 cm from the plucking position, a Telecaster pickup (electrically loaded with 110 kΩ // 330 pF) was mounted below the string. The integral of the pickup voltage is shown in Fig. 1.24 in normalized fashion. The flexural wave passes the pickup 1 ms after its generation and induces a voltage there. The dilatational wave that is also generated runs along the string, is reflected, and arrives back at the bearing after 5,2 ms. Here, a secondary flexural wave is generated (among other waves) that passes the pickup after another millisecond. In Fig. 1.24, the maximum of this secondary impulse reaches almost 40% of the magnitude of the primary impulse. At least for this experimental setup, this is an impressive testimony for the significance of the dilatational wave.

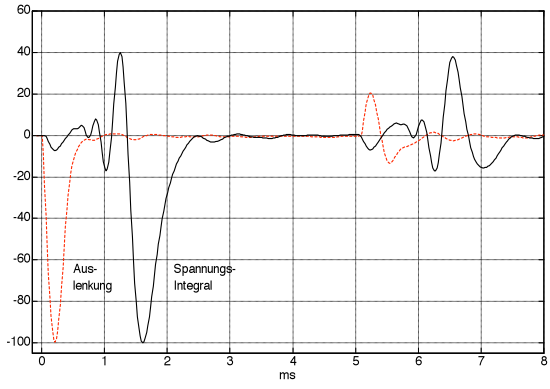

Fig. 1.24: Measurments with a magnetic pickup. "Auslenkung" = displacement; "Spannungsintegral" = voltage integral